Hindawi
Geofluids
Volume 2022, Article ID 3749343, 12 pages
https://doi.org/10.1155/2022/3749343

Research Article

Experimental Study on Shear Strength of Root Composite Tailing Soil Based on Interfacial Bonding

Qing Chao Yang,[1,2] Zhe Hao,[3] Sheng You Lei,[1] Yan Chen,[2] Hong Xia Shen,[4] Ying Zhang,[5,6,7] Qian Zhang,[5,6,7] and Da Teng[5,6,7]

[1]*School of Highway, Chang'an University, Xi'an 710064, China*
[2]*School of Highway and Architecture, Shandong Transport Vocational College, Weifang 261206, China*
[3]*College of Environmental Sciences, Liaoning University, Shenyang 110036, China*
[4]*Shandong Textile Architecture Design Institute Co., LTD, Jinan 250013, China*
[5]*Liaoning Nonferrous Geological Exploration and Research Institute Co, Shenyang 110013, China*
[6]*Liaoning Provincial Key Laboratory of Mine Environment Geotechnical Engineering, Shenyang 110013, China*
[7]*Technology Innovation Center for Old Mine Geological Disaster Prevention and Ecological Restoration, Ministry of Natural Resources, Shenyang 110013, China*

Correspondence should be addressed to Zhe Hao; 2017021004@chd.edu.cn

Received 6 June 2022; Accepted 12 August 2022; Published 5 September 2022

Academic Editor: Zhengzheng Xie

At present, the root soil interface bonding is not considered in the root system of mechanical soil-fixing model. The typical restoration plant Amorpha fruticosa, utilizing the widely used Wu model (WWM), the tensile and tensile properties of single root, and the shear strength properties of root soil composite tailing, is analyzed by the tensile tests of plant roots, pullout tests, and shear tests based on the effect of interfacial bond strength; based on the failure mode of root system in root soil, the modified WWM model is used to calculate the increment of shear strength of composite tailing soil. The results showed that ① the relationship between root diameter of A. fruticosa and tensile strength was power function. ② The bond between root and soil becomes more tight, and the pullout strength of the root system increases significantly. ③ When root soil area ratio (RAR) is the same, shear deformation capacity of root soil composite tailing soil increases with the increase of interface bonding strength. Under the condition of the same interface bonding strength, the cohesion of root soil composite tailing soil is greater than that of tailing soil and increases with the increase of RAR, but the change of internal friction angle is not significant. When the pullout strength is added to the plant root prediction model, the soil consolidation effect of the plant root system can be better reflected. The range of the revised coefficient of the WWM model for the root soil composite tailing soil is 0.15~0.37. The research results will provide a theoretical basis and data support for quantifying the ecological restoration and reinforcement capacity of tailing pond shrubs and plants, slope stability, soil and water management, and other ecological soil consolidation capacity of mines.

1. Introduction

Open-pit mining of mineral resources destroys local vegetation and pristine terrain. The abandoned tailing in tailing ponds seriously endangers the safety of people's lives and properties and the surrounding ecological environment [1, 2]. Tailing ponds are even the focus of ecological environment management in the mines. The core content of the management of tailing dams is the stability and ecological restoration of tailing dam slopes [3], which can effectively solve or alleviate the problems of tailing dam slope failure [2, 4], landslide accidents [5, 6], heavy metal pollution [7], and vegetation restoration [8].

The mechanical soil consolidation effect of plant roots is controlled by multiple factors, such as the spatial distribution characteristics of root parameters such as root number, length, surface area, root bulk density and root angle with soil

[9, 10], root tensile and pullout mechanical properties [11], root surface roughness, soil particle arrangement and pore development characteristics, and other microstructural characteristics [12, 13]. All of the above factors have an impact on the vegetation-enhanced friction characteristics and soil consolidation effects. Therefore, analyzing and quantifying the root consolidation effect is a hot and difficult area of current research. Wu et al. [14] established the Wu model (WWM) to quantify the root effect on soil shear strength by assuming that all root systems can reach the maximum tensile strength and break at the same time [15, 16]. Studies have shown that the shear strength of plant roots calculated by the WWM model deviates significantly from the actual values [17–19] and the WWM model needs to be corrected [20, 21]. Due to their simple parameters and high applicability, WWM models have been widely used to evaluate the effect of root consolidation [15, 22], but all lack the analysis of interfacial cohesion effects. Therefore, it is important to carry out experimental research on the shear strength of root composite tailing soil based on interfacial adhesion.

At present, the influence of root soil interface adhesion strength on the shear strength of root soil composite and its variation law need to be further studied. In particular, the experimental study of shear strength considering root soil adhesion in the complex environment of open tailing has not been carried out. In this paper, A. fruticosa was used as the test object in the ecological restoration area of Crooked Head Mountain tailing dam in Liaoning Province, China. The effect of adhesion between the root soil interface on its shear strength was analyzed by root tensile, pullout, and direct shear tests. It compares the predicted values of WWM model with the experimental results. It uses correction factors to quantify the root soil interfacial adhesive action and improve the model prediction accuracy and to provide theoretical support and practical application support for tailing ecological restoration and vegetation slope protection.

2. Research Content and Methods

2.1. Test Materials

2.1.1. A. fruticosa Root System. The sampling site of the test material was the second valley-type tailing dam of Xiao Xi Gou in Crooked Head Mountain iron ore mine of Ben steel Group. A. fruticosa is a typical representative plant for the ecological restoration area of the outer slope of the tailing dam. The test was conducted in August 2021 at Crooked Head Mountain, where a 4-year old planting time of A. fruticosa dam slope platform was selected. Thirty well-grown plants were randomly selected on the platform, and the height (122.6 ± 26.6 cm), crown width (125.5 ± 15.4 cm), and ground diameter (2.0 ± 0.5 mm) of the standard plants were measured. Test samples were selected according to the standard strains for whole plant collection. The root system was dug out from the center of the plant to prevent water loss. Roots and soil were quickly wrapped and transferred to the laboratory. The roots were placed in the refrigerator at 4 for cold storage for subsequent tests. The root system of A. fruticosa on the site is shown in Figure 1.

Figure 1: Root diagram of tailing pond plants.

According to the cumulative characteristics of root diameters of A. fruticosa [23], root diameters accounting for more than 85% of the total root diameter class were concentrated in the range of 0.5 to 4.5 mm, with roots in the range of 1.5 to 2.5 mm being the most prominent. Therefore, roots in the range of 0.5~4.5 mm were selected as the root systems for tensile strength tests. Considering the limitation of the test box size in laboratory drawing friction test and straight shear test, the root of A. fruticosa with uniform diameter, good growth, and diameter of 2 mm ± 0.1 mm was selected as the root material for the test.

2.1.2. Tailing Soil. The tailing soil without plants in the tailing area was taken to the test room. The tailing soil was air-dried and baked at 105 °C for 8 h. It was passed through a 2 mm sieve and sealed in a sealing bag to prepare root soil composite tailing. Table 1 shows the physical index of tailing soil. Figure 2 shows the gradation curve of tailing soil.

2.2. Determination of Root Soil Interfacial Bond Strength Gradient. Since there are few studies on root soil interfacial bond strength, this paper combines the findings of previous tests on root soil interfacial bond strength and commonly used binder materials investigated in literature [24–31], as shown in Table 2. The results of liquid sodium silicate and cyanoacrylate simulated root soil interfacial bond strength tests were obtained by direct shear friction pretest, which satisfied the statistical root soil interfacial bond strength test (1.1~28.3 kPa range). Therefore, in this paper, three kinds of root soil interfacial bond strength test conditions were designed using liquid sodium silicate and cyanoacrylate, and the entire root system skin layer was uniformly coated with liquid sodium silicate and cyanoacrylate for the pullout friction test of A. fruticosa root system + tailing soil (RS), A. fruticosa root system + liquid sodium silicate + tailing soil (NRS), and A. fruticosa root system + cyanoacrylate + tailing soil (GRS). Considering the relatively small burial depth of the root system, a uniform distribution of the interfacial adhesive strength was assumed during the pulling process [26, 27].

$$P_{\max} = f(D) = \pi D L \tau, \tag{1}$$

where $P_{\max}$ is the maximum pullout force (N); D is the diameter (mm); L is the root burial length (mm); and τ the root soil interface pullout shear stress is a set to the root soil interface shear strength (kPa) [27].

Table 1: Basic physical parameters of tailing soil.

Natural water content	Natural density	Particle density	Natural porosity ratio	Plasticity index	Liquidity index
w/%	$\rho/(g{\cdot}cm^{-3})$	G_s	e_0	IP	IL
9.6	1.94	2.71	0.69	14.3	0.15

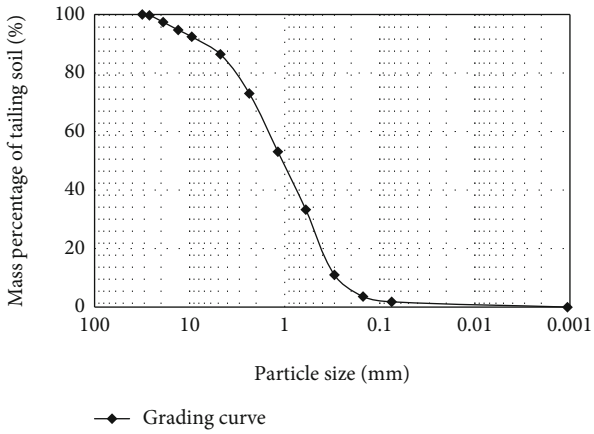

Figure 2: Grading curve of tailing soil.

Based on the root damage pattern and interfacial adhesion effect, three different interfacial adhesion strength gradients of 1.5, 1.6, and 1.7 were determined for RS, NRS, and GRS adhesion gradients.

2.3. Specimen Preparation and Method

2.3.1. Tensile Test. ① Root system selection: The root diameter in the range of 0.5-4.5 mm was graded at 0.5 mm intervals. Each diameter grade cut side must take 5-10 roots, root length of about 120 mm, each end reserved 20 mm, and the actual tensile length of the root system 80 mm ± 2 mm to do tensile specimens

② Test method: The tensile device consists of Edberg digital display push-pull meter (ZP-1000N, ±0.5%), tensile frame, displacement scale (WD-180 mm, ±0.01 mm) and signal collection device, as shown in Figure 3(a). During the loading process, manual loading was used and the effect of loading rate was neglected [32]. The push-pull apparatus was connected to a computer to obtain the tensile data. To ensure the accuracy of the test data, only the tensile test data at the middle fracture 1/3 position were retained during the test, as shown in Figure 3(b)

2.3.2. Straight Shear Test

(1) Tailing Soil Sample Preparation. The natural moisture content of tailing soil in the study area was 9.6%. To facilitate the calculation, the water required for the test was calculated according to the 10% water content of the tailing soil. After stratified spraying and uniform mixing, the tailing soil was sealed as test sample soil for reserve.

(2) Root Soil Complex Tailing Soil Sample Making. ① Tailing soil specimen preparation method: Prepare tailing soil samples with 10% moisture content in advance, and compact them in two layers with compaction hammers, keeping the same number of times for each layer. When the compaction of the two layers is completed, the compaction cylinder is removed, and the tailing soil (TS) specimen is prepared with a ring knife

② Root soil composite tailing soil specimen preparation method: A. fruticosa root system was selected with a diameter of 2 mm, and 20-mm-long uniform diameter sections were intercepted and set aside, using the vertical root distribution method. Soil samples are weighed and prepared using two layers of compaction. After the first layer of tailing soil was put into the ring knife, the whole root system was coated with liquid sodium silicate and cyanoacrylate evenly, and the first layer of compaction was carried out after the root system was inserted. Due to the toughness of the root system, after the first layer of soil compaction was completed, the upper surface root system was gently added up with forceps. A second layer of compacted tailing soil sample was added, and the root system was gently straightened with tweezers for the second compaction. According to the test protocol, the RS, NRS, and GRS samples were sealed in plastic wrap. The samples need to be placed in a constant temperature and humidity maintenance box for 24 h. Table 3 shows sample numbers and related parameters. Tailing soil and A. fruticosa root soil composite tailing soil specimens, as shown in Figure 4

The root content in the soil is described in terms of the root cross-sectional rate, RAR, which is given by the following equation:

$$RAR = \sum_{i=1}^{n} \frac{A_R}{A_S}, \tag{2}$$

where A_S is the soil cross-sectional area (mm^2), A_R is the root area (mm^2), and n is the number of root systems.

③ Test method: Using ZJ straight shear to conduct the test, the rate of 0.8 mm/min was applied to four specimens with 100, 200, 300, and 400 kPa normal pressure, respectively

2.3.3. Plant Root Pullout Test. The test was performed using an Edelbrock digital push-pull meter (see Section 2.3.1 for model details) and a cylindrical (400 mm in height and 100 mm in diameter) test box. The test box was fixed with card buckles at three positions to the base to ensure the position of the test box was fixed for each pulling test. In the test preparation process, A. fruticosa root diameter was selected as 2 mm, length was 100 mm, and the jig end was left 20 mm. the A. fruticosa root system was buried horizontally in the cylindrical test box with a burial length of 80 mm ± 2 mm. The compaction was completed in two layers. After the first layer of soil

Table 2: Statistics of common binder materials.

Binder name	Viscosity index/pa.s	Notes
Water-based polymer-isocyanate wood adhesives	≥0.1	Tensile shear strength ≥ 1.2 Mpa
Neoprene-based adhesives	2~8	Tensile shear strength ≥2.2 Mpa
Natural rubber-based adhesives	0.4~2.5	—
Liquid sodium silicate	0.024~0.18	Baume degree 40, modulus 3.3
Cyanoacrylate	0.3~6	—
Polyvinyl acetate emulsion wood adhesives	0.5	Compression shear strength 3~10 Mpa

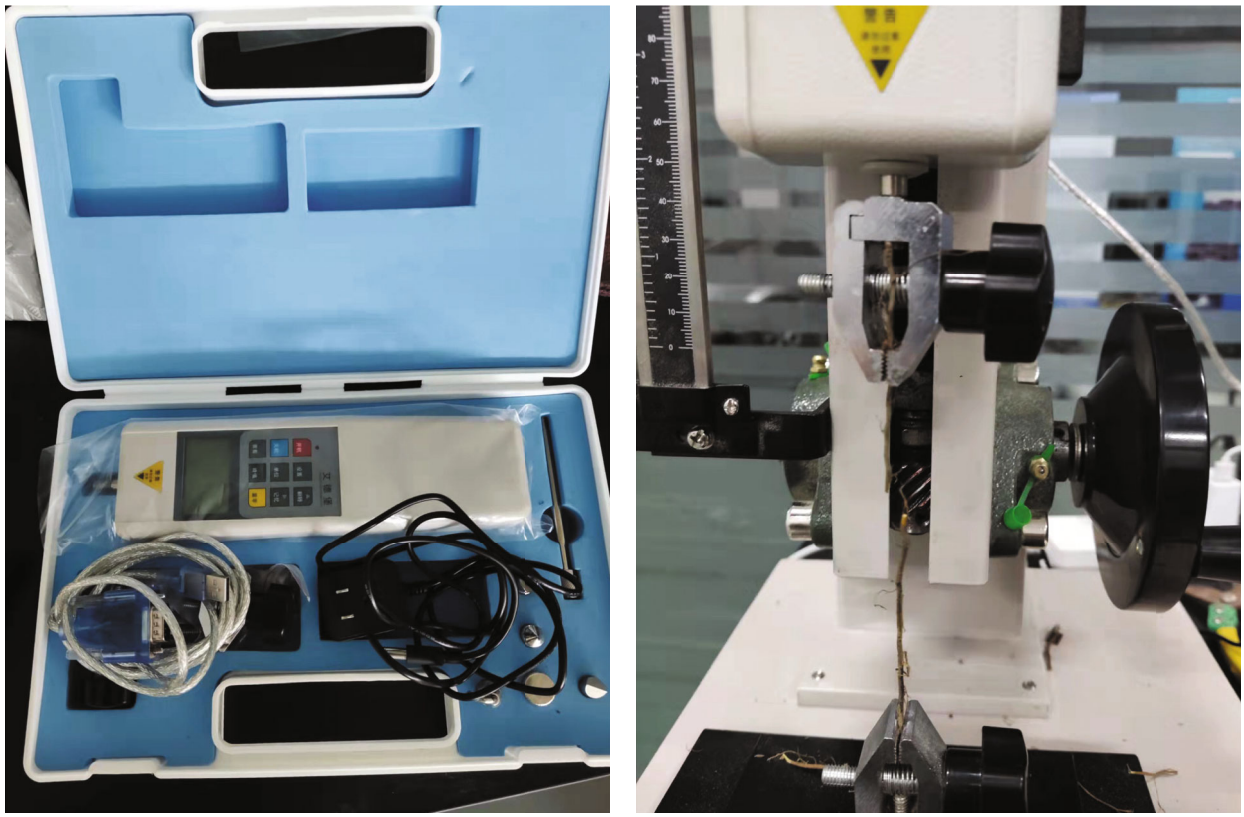

(a) Drawing test device (b) Pull out test of A. fruticosa root

Figure 3: Root pulling test of A. fruticose.

Table 3: Sample number and parameters.

No.	Types	D/mm	RAR	Binding materials	Material properties
1	TS	2	0	0	0
2	RS	2	0.21, 0.42, 0.63	0	0
3	NRS	2	0.21, 0.42, 0.63	Liquid sodium silicate	Baume degree 40, modulus 3.3
4	GRS	2	0.21, 0.42, 0.63	Cyanoacrylate	Viscosity 6 pa.s

is completed with compaction and scraping, the root epidermis should be uniformly coated with liquid sodium silicate and cyanoacrylate according to the test protocol. The second layer of compaction is performed after the roots are placed freely through the opening of the test box. The samples need to be sealed in plastic wrap and placed in a constant temperature and humidity maintenance box for 24 h. The root pullout resistance device is shown in Figure 5.

3. Test Results

3.1. Tensile Properties. From Figures 6 and 7, the average diameter of A. fruticosa increased from 0.87 ± 0.12 mm to 3.75 ± 2.11 mm, and the tensile strength increased from 28.24 ± 17.06 N to 108.93 ± 43.23 N. The tensile strength increased as a function of the root diameter. The tensile strength decreased from 45.21 ± 16.13 MPa to 8.13 ± 3.26

(a) Tailing soil (b) A. fruticosa root composite tailing soil

Figure 4: Composite tailing soil samples of tailing soil and A. fruticosa root soil prepared.

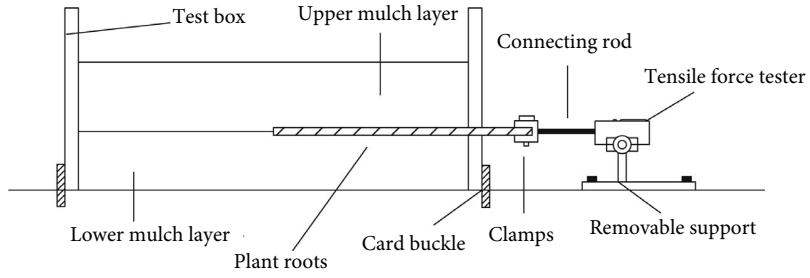

Figure 5: Root pulling test device.

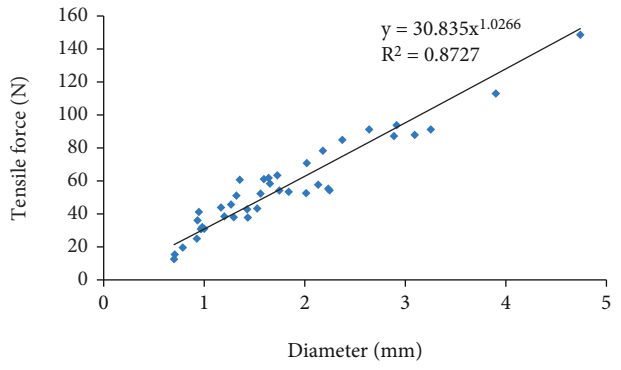

Figure 6: Relationship curve between root tensile resistance and diameter of A. fruticose.

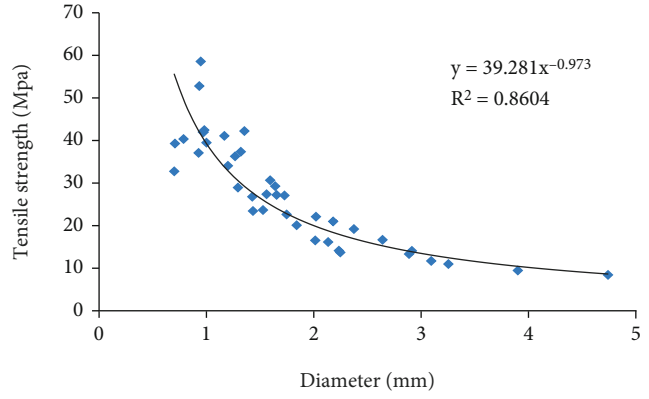

Figure 7: Relationship curve between tensile strength and diameter of A. fruticosa root system.

MPa, and the tensile strength decreased with the increase of root diameter as a power function.

3.2. Pulling Mechanical Properties. Figure 8 shows the pulling time-tension curves of the root system at different interfacial bonding strengths.

As can be seen from Figure 8, at the initial stage of force, elastic deformation occurs between the roots and soil particles and soil particles without sliding due to the small displacement. With the increase of tensile force, the root system embedded in the soil bonded more tightly under the effect of root soil interface bond strength, and the pullout resistance increased approximately linearly and reached the peak. According to Figure 8, the peak of the curve was extracted, and GRS (48.5 N) > NRS (22.5 N) > RS (16 N) was obtained. When the tension reaches the maximum root soil interface static friction, the root soil has not yet moved due to the interfacial adhesion, and a root soil anchorage zone is formed, as shown in Figure 9. When the soil particles on the boundary of the anchorage area start to slip, the interfacial friction gradually decreases. At this time, the root pullout force consists of the friction between the root soil interface and the friction between soil particles on the boundary of the anchorage zone.

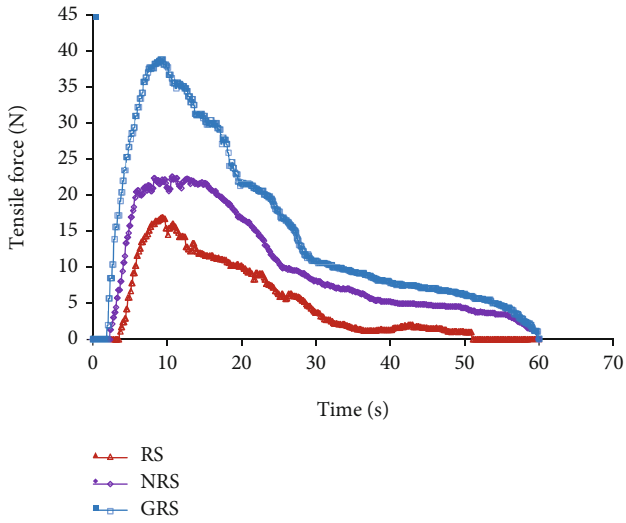

Figure 8: Root pulling time tensile curve under different interfacial bonding strength.

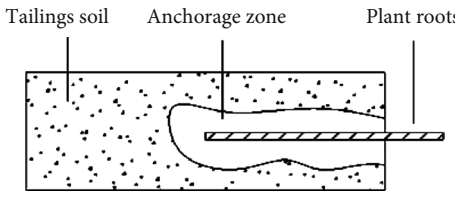

Figure 9: Schematic diagram of root soil interface.

The new root soil friction interface is formed with the rearrangement of soil particles during the dynamic pullout of the root system, and the anchorage effect gradually decreases and tends to zero.

3.3. Direct Shear Test Considering the Effect of Interfacial Bonding Strength

3.3.1. Relationship Between Stress and Displacement for Different Interface Bonding Strength. Figure 10 shows the stress and displacement relationship curve between tailing soil and the composite tailing soil of A. fruticosa root with RAR of 0.42.

As can be observed in Figure 10, the curve first undergoes elastic deformation. With the increase of shear stress, the strain produces plastic deformation. The curve line was nearly horizontal after shear damage, and the elastic-plastic characteristics were significant. Shear deformation resistance of A. fruticosa root soil composite tailing soil specimens were all significantly stronger than TS. At the 400 kPa, the shear displacements of RS, NRS, and GRS root soil composite tailing soil were 2.39 mm, 2.46 mm, and 2.65 cm, respectively. The shear displacement of tailing soil TS was 2.06 mm. Compared with the shear displacement of tailing soil, the increases of shear displacement of RS, NRS, and GRS root soil composite tailing soil were 16.01%, 19.42%, and 28.64%, respectively. The shear displacement of RS, NRS, and GRS composite specimens under the same pressure and stress are more important than that of TS. It reflects that to a certain extent, the interfacial bonding strength can enhance the shear strength of the soil.

3.3.2. Comparison of Shear Index under Different Bonding Strength Conditions

(1) Cohesive. The results of cohesion and growth of tailing soil and A. fruticosa root tailing soil specimens are shown in Table 4. The cohesion of A. fruticosa root tailing soil is greater than 15.08 of TS. The cohesion tends to increase with the increase of cohesive strength when the RAR is the same. For example, for RAR of 0.21, the increase in cohesion was GRS (15.78%) > NRS (14.66%) > RS (10.48%) compared with TS specimens. When the root soil cohesive strength was the same, the root soil composite tailing soil cohesive force showed an increasing trend with the increase of RAR. When the RAR was maximum, the root soil composite tailing soil cohesion increased the most. For example, GRS with the increase of RAR, the increase of the cohesive force of root soil composite tailing soil adhesion of purple acacia was 15.78%, 41.58%, and 78.91%. The results show that RAR can significantly enhance the cohesion of tailing soil under three interfacial bonding strength gradients.

(2) Angle of Internal Friction. Table 5 shows the angle of internal friction and the growth of the specimens.

From Table 5, the internal friction angles of the tailing soils of root A. fruticosa are all greater than 26.35° of TS. However, with the increase of interface bonding strength and RAR, the change of internal friction Angle was not significant. For example, when RAR was 0.21 and 0.63, the internal friction angle of A. fruticosa root tailing shows an increasing trend with the increase of bonding strength, and the increase was GRS > NRS > RS. However, when RAR was 0.42, the increase of GRS internal friction angle was the smallest. The effect of root soil interface adhesion strength on the internal friction angle was not significant. This is consistent with the results of Lian, et al. [33], Normaniza, et al. [34], and Li, et al. [35].

3.4. Comparison of Measuring and Modeled Values of Root System Additional Cohesion

3.4.1. WWM Model. Part of the shear force under the action of shear force is transferred to the plant roots, and the root system bears the tensile force, which is equivalent to the increased cohesion, and WWM model quantified the shear strength of soil reinforced by roots.

$$C_r = 1.2T_R\left(\frac{A_R}{A_S}\right), \tag{3}$$

where T_R is tensile strength (MPa) and C_r is shear strength increment (kPa).

3.4.2. Correction Model of Root Soil Composite Tailing Soil Based on the Effect of Interfacial Adhesive Strength. In the actual shear damage process, not all roots are pulled out at

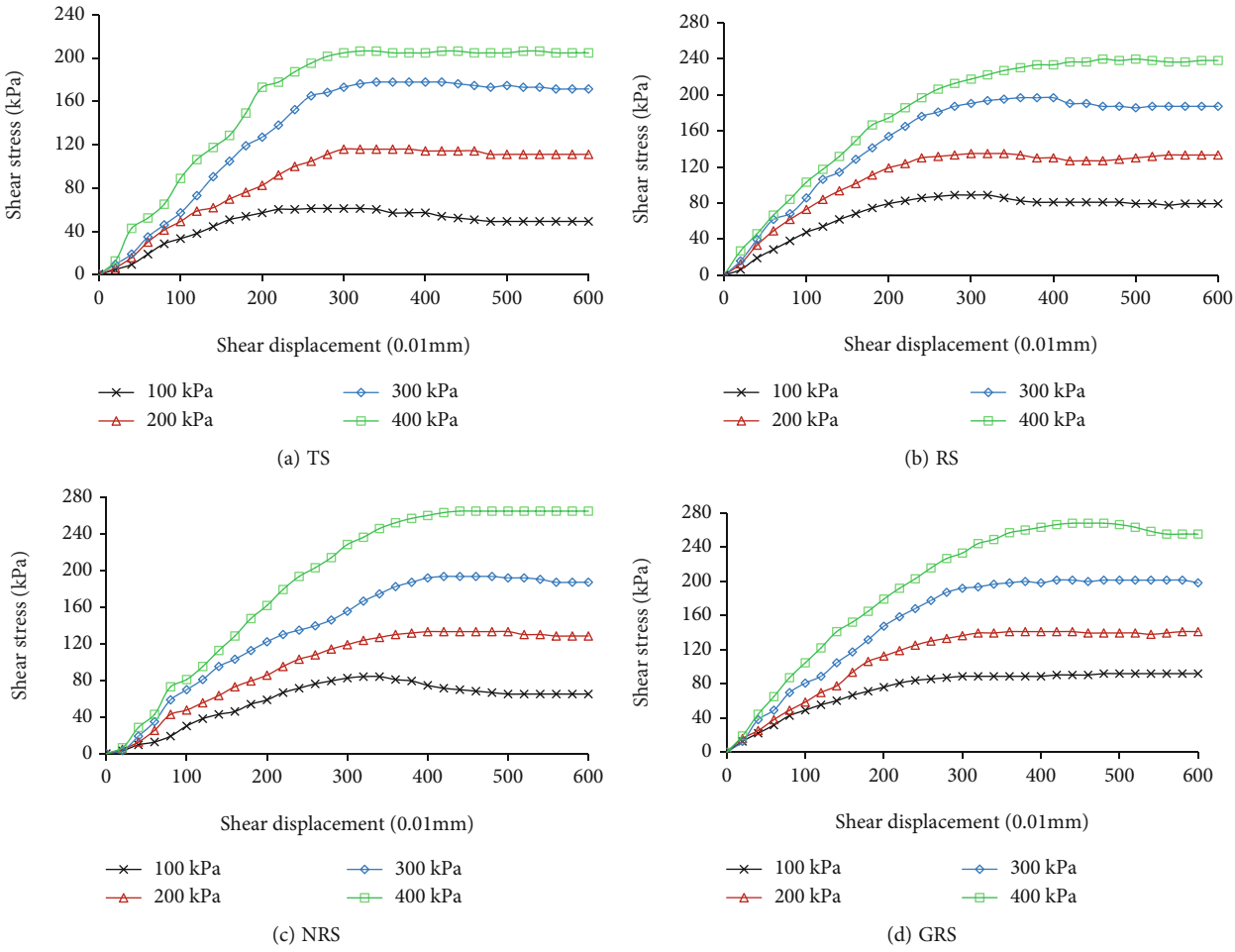

Figure 10: Stress and displacement curves of samples.

Table 4: Cohesion and growth range of sample.

Types	RAR = 0.21		RAR = 0.42		RAR = 0.63	
	Cohesion/kPa	Increase in cohesion/%	Cohesion/kPa	Increase in cohesion/%	Cohesion/kPa	Increase in cohesion/%
RS	16.66	10.48	20.39	35.21	26.18	73.61
NRS	17.29	14.66	20.63	36.80	26.25	74.07
GRS	17.46	15.78	21.35	41.58	26.98	78.91

Note: The cohesive force of tailing soil is 15.08 kPa.

Table 5: Internal friction angle and growth range of sample.

Types	RAR = 0.21		RAR = 0.42		RAR = 0.63	
	Angle of internal friction/(°)	Angle of internal friction increase/%	Angle of internal friction/(°)	Angle of internal friction increase/%	Angle of internal friction/(°)	Angle of internal friction increase/%
RS	28.89	9.64	30.21	14.65	30.69	16.47
NRS	29.34	11.35	31.82	20.76	31.14	18.18
GRS	30.22	14.69	29.42	11.65	31.56	19.77

Note: The internal friction angle of the tailing soil is 26.35°.

the same time, but some roots are pulled out. Therefore, this paper corrects the pullout strength corresponding to the root pullout damage in order to accurately quantify the value of root soil cohesion enhancement effect under the action of cohesive strength. The correction factor k is introduced to obtain.

$$C_r = k \times 1.2 T_P \left(\frac{A_R}{A_S}\right). \tag{4}$$

Table 6: Calculation results of measured value and model value of root additional cohesion.

Types	RAR	Measured value			Predicted value of WU model		Modified WU model predicted value k		k
		Tensile strength/MPa	Pulling strength/MPa	Shear strength amount of increase/kPa	Shear strength amount of increase/kPa	Growth rate/%	Shear strength amount of increase/kPa	Growth rate/%	
RS	0.21	16.15	5.10	4.58	40.70	788.60	12.84	180.37	0.36
	0.42	16.15	5.10	5.21	40.70	681.15	18.06	246.59	0.29
	0.63	16.15	5.10	6.38	40.70	537.90	38.92	386.81	0.21
NRS	0.21	16.15	7.17	8.31	81.40	879.49	25.68	209.04	0.32
	0.42	16.15	7.17	8.55	81.40	852.00	36.11	322.39	0.24
	0.63	16.15	7.17	9.27	81.40	778.06	77.85	570.09	0.15
GRS	0.21	16.15	12.32	14.10	122.09	765.91	38.52	173.21	0.37
	0.42	16.15	12.32	14.17	122.09	761.64	54.17	282.30	0.26
	0.63	16.15	12.32	14.90	122.09	719.42	116.77	525.34	0.16

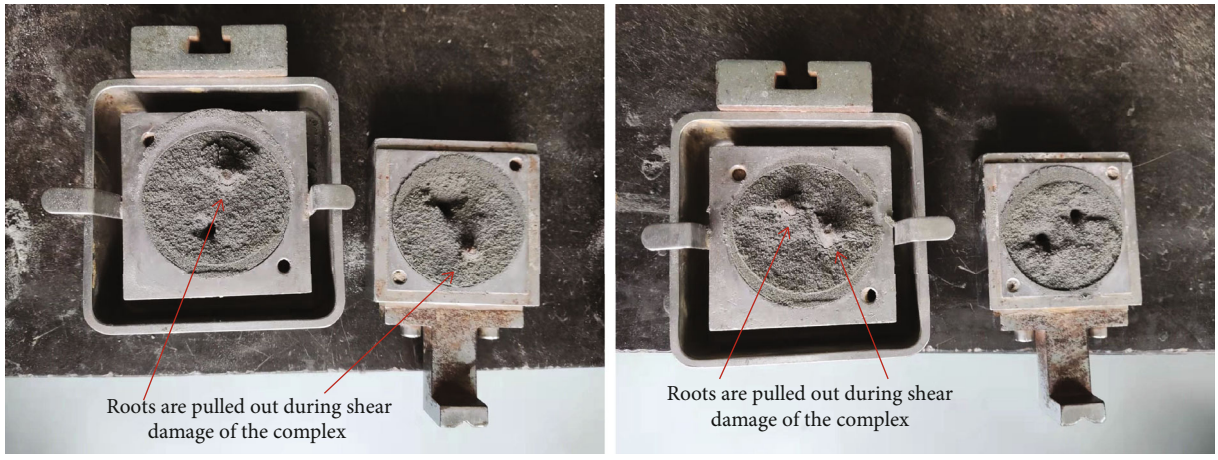

Figure 11: Shear test of A. fruticosa root soil composite tailing soil.

The correction factor k was derived by comparing the model quantified root cohesion (ΔC_w) results with the root cohesion (ΔC_d) results from the shear test considering the effect of adhesive strength:

$$k = \frac{\Delta C_d}{\Delta C_w}. \quad (5)$$

From the measured values of root additional cohesion and model values calculated in Table 6, it is clear that the WWM model overestimates the reinforcement effect of plant roots [21, 36]. The predicted values of shear strength of A. fruticosa root tailing soil predicted with the WWM model were 5.37 to 8.79 times higher than the measured values. And the predicted values with the modified model were 1.80-5.70 times of the measured values. The results indicate that it is more reasonable to fully consider the root soil interface cohesive effect in the model than to estimate the root shear strength directly using the root tensile strength. The range of model correction factors for the three types of cohesive strengths compared ranged from 0.15 to 0.37. The WWM model correction factors were different because in the calculation using the WWM model, it was assumed that all the roots on the shear surface broke simultaneously and the root reinforcement capacity was fully reflected. However, under the test conditions, most of the roots slipped out of the soil instead of breaking when the shear damage occurred in the composite, as shown in Figure 11, making some of the root reinforcement capacity could not be fully developed. Meanwhile, the main root of A. fruticosa had a large diameter and did not break during shearing. This is the main reason for the small correction factor.

4. Mechanism Analysis of Influence of Plant Roots on Soil Shear Strength with Different Interfacial Adhesion Strengths

4.1. Mechanism of Root Soil Contact Surface Interaction. The interaction between rootless soil mainly comes from the inter-soil adhesion, friction between soil particles, and the embedded locking force formed by the soil and rough bumps [37]. The initial elastic shear deformation at the interface is mainly the soil compaction deformation under

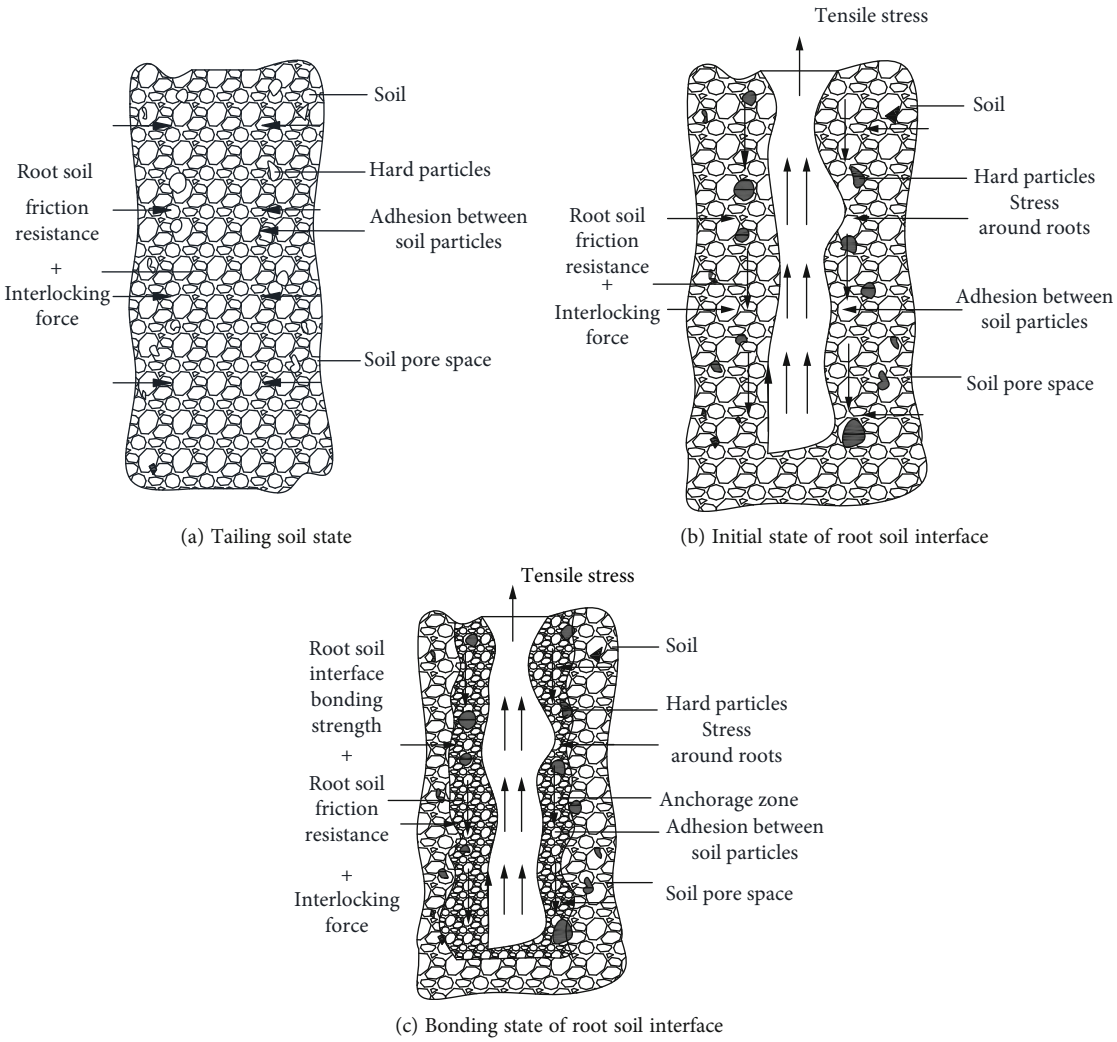

Figure 12: Schematic diagram of interface action between tailing soil and root soil.

shear loading. Local plastic deformation occurs under the interaction of soil particles, leading to shear damage, as shown in Figure 12(a). The root soil interaction in the initial state mainly relies on the action of the adhesion between soil particles, the frictional force between soil particles and the root surface, and the embedded locking force between the soil and the concave and convex surfaces of the root system, as shown in Figure 12(b). A. fruticosa during root growth and fungi such as rhizobia are present around the roots, and some gelatinized chemicals are secreted on the root surface to form interfacial chemical adhesion [25, 38]. The irregular connection between root and soil interface is strengthened, and the whole combination of root and soil particles can be formed gradually. Similar to soil cohesion, the interaction between soil particles and root surface forms interfacial soil cohesion. When the A. fruticosa root complex tailing soil is subjected to external forces, the forces are transmitted to the plant root fibers with tensile strength because the root soil interface has good transmission properties. The gradual dispersion of the acting force produces an anchoring region consisting of interfacial adhesion, interfacial frictional resistance, and embedded locking force, which makes the strength of the purple locust root composite tailing soil enhanced, as shown in Figure 12(c).

When the soil containing roots is subjected to shear, the root system converts the internal shear stress of the soil body into the tensile stress it is subjected to through the root-soil interface adhesion. The root system tension, root-soil interface adhesion, and soil shear force act together to mechanically reinforce the shear strength of the soil on the slope. Thus, the mechanism of root-soil contact surface interaction and shear deformation damage process can be summarized as showed in Figure 13 [39].

At the initial stage of shear deformation, the interaction between the rough contact surface of the tailing soil and the root system is dominant, and the contact surface produces extrusion deformation. After the tailing soil is squeezed, the root-soil complex formed by the root system and the adjacent soil is uniformly distributed throughout the interface. The increase of root density makes the contribution of roots to the shear properties of the interface gradually appear. After entering the dynamic friction stage, the root system and soil body act together to resist the shear load. Based on the gradual development of soil shear resistance,

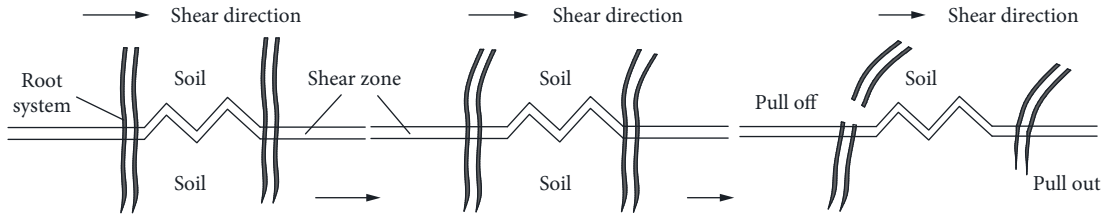

Figure 13: Schematic diagram of the mechanism of root-soil contact surface action and progressive damage process.

the reinforcing effect of the root system in the soil and the anchoring effect of the interface also gradually comes into play. The anchoring effect of the root system mainly depends on the ultimate tensile force of the root system itself, the interfacial adhesion, and the interfacial friction.

When the ultimate pullout force of root system, interfacial adhesion and interfacial friction play together to reach the limit, the shear stress borne by the root system reaches the peak. The larger the RAR, the more obvious the contribution to the interfacial shear stress. With further shearing, the root system is successively pulled off or pulled off, and the interfacial shear stress gradually decreases. In the actual situation, the damage of the root system in the root-bearing soil is not all in the form of pull-off or pull-out damage, but part of the root system is pulled off, and part of the root system is pulled out. The root-soil interface bonding strength is between the maximum and minimum values [24]. The root system pull-off or pull-out damage shows the characteristic of progressive damage [39].

4.2. The Influence of Interfacial Bonding Strength on the Cohesion of Root Soil Composite. The influence mechanism of interface bonding strength on the cohesion of root soil composite tailing soil is mainly reflected as follows: (1) when the soil is subjected to external forces, the voids existing in the soil continue to expand and produce cracks. And the root system embedded in the soil body can fill certain cracks. It effectively restrains the expansion of plastic cracks, improves the crack-blocking enhancement of the complex, and increases the cohesion of the root soil complex. (2) The gelling material secreted by the root system can directly increase the thickness around the soil particles. The concave and convex structures on the surface of soil particles form an effective adhesion and embedding effect with the root system, forming a bond with certain integrity. This increases the root soil specific surface area, reflecting that the root soil interface adhesive strength effect can increase the cohesive of the root soil composite. (3) A. fruticosa is a taproot type. The root system is distributed in the soil body approximately vertically. Each root segment of the root soil complex can anchor the soil through the shear surface and promote the transfer and diffusion of shear stress.

5. Conclusion

This paper is based on the WWM model. Through tensile, pullout, and shear tests, the effect of root soil interfacial adhesion is fully considered. It determines the model correction coefficient, which quantifies the shear strength characteristics of root soil composite tailing soil with different interfacial bonding strength, leading to the following conclusions:

(1) The root tensile strength of Amorpha fruticosa increased as a power function of the increase of the root diameter of A. fruticosa, and the tensile strength decreased as a power function of the increase of the root diameter of A. fruticosa. As the bonding strength between the root system and the tailing soil body of A. fruticosa increased, the bonding between the root-soil became tighter and the root pullout resistance increased significantly, in the order of GRS (48.5 N), NRS (22.5 N), and RS (16.0 N)

(2) The shear strength of root soil composite tailing soil of purple locust was significantly higher than that of tailing soil, and the root system could significantly enhance the soil shear strength; with the increase of interfacial adhesive strength, the shear deformation resistance of root soil composite tailing soil was enhanced; when the root soil area ratio was the same, the higher the interfacial adhesive strength, the greater the cohesive force; when the interfacial adhesive strength was the same, the cohesive force increased with the increase of root soil area ratio, but the change pattern of internal friction angle is not significant

(3) The model of modified WWM model fully considered the effect of root soil interfacial cohesion, and it was more reasonable to calculate the root pullout force than to estimate the shear strength directly using the root tensile strength, and the variation range of the model correction coefficient was 0.15~0.37

(4) When the root soil is subjected to shear, the root system uses the root soil interface adhesion to convert the soil shear stress into the tensile stress it is subjected to, and the root tensile force, root soil interface adhesion, and soil shear force act together to achieve the enhancement of the soil shear strength

Data Availability

The data used to support the findings of this study are available from the corresponding author upon request.

Conflicts of Interest

No potential conflict of interest was reported by the authors.

Acknowledgments

The research was supported by the Major Science and Technology Program for Water Pollution Control and Treatment, China (no. 2015ZX07202-012), the Project of Natural Science Foundation of Liaoning Province, China (No. 20180550192), the Liaoning Bai Qian Wan Talents Program, China (no. [2015]33), the Project of Science and Technology of Liaoning Province, China (no. 2019JH8/10300107 and no. 2020JH2/10300100), and the special project of guiding local scientific and technological development by the Central Government of Liaoning Province (no. 2021JH6/10500015).

References

[1] Y. P. Yang, P. S. Huang, and G. G. Chen, "Safety evaluation of tailing pond based on FIM-optimization unascertained measure," *Journal of Safety and Environment*, vol. 21, no. 3, pp. 996–1004, 2021.

[2] Y. Witasari, E. K. Helfinalis, and W. Prayogo, "Characteristics of deposited mine tailing on the Senunu Canyon, Indonesia," *IOP Conference Series: Earth and Environmental Science*, vol. 789, no. 1, article 12018, 2021.

[3] Y. N. Liu, R. Q. Huang, E. L. Liu, and F. Hou, "Mechanical behaviour and constitutive model of tailing soils subjected to freeze-thaw cycles," *European Journal of Environmental and Civil Engineering*, vol. 25, no. 4, pp. 673–695, 2021.

[4] T. Haruka, F. Kazunori, and M. Akira, "A Mohr-Coulomb-Vilar model for constitutive relationship in root-soil interface under changing suction," *Soils and Foundations*, vol. 61, no. 3, pp. 815–835, 2021.

[5] M. Ogilvie Cameron, B. V. Ashiq Waqar, and B. A. Hiteshkumar, "Quantifying root-soil interactions in cover crop systems: a review," *Agriculture*, vol. 11, no. 3, pp. 218–218, 2021.

[6] Y. J. Zhao, X. S. Hu, H. T. Li, C. Y. Liu, G. R. Li, and H. L. Zhu, "Characteristics of slope soil shear strength reinforced by shrub roots in cold and arid environments," *Agricultural Engineering*, vol. 32, no. 11, pp. 174–180, 2016.

[7] J. Tia, J. N. Ji, Q. Zhong, P. C. Yu, L. J. Yang, and B. Yuan, "Analysis on improvement of slope stability in root soil composite of Picea crassifolia forest in Helan Mountain," *Editorial Office of Transactions of the Chinese Society of Agricultural Engineering*, vol. 33, no. 20, pp. 144–152, 2017.

[8] Z. Long, H. Zhu, H. Bing et al., "Predicting soil cadmium uptake by plants in a tailings reservoir during 48-year vegetation restoration," *Science of The Total Environment*, vol. 818, article 151802, 2022.

[9] Y. Z. Wang, X. F. Liu, Z. K. Zhang, D. G. Ma, and Y. Q. Cui, "Experimental research on influence of root content on strength of undisturbed and remolded grassroots-reinforced soil," *Rock and Soil Mechanics*, vol. 37, no. 8, pp. 1405–1410, 2015.

[10] G. Q. Kong, L. Wen, H. L. Liu, and C. Q. Wang, "Strength properties of root compound soil and morphological observation of plant root," *Rock and Soil Mechanics*, vol. 40, no. 10, pp. 3717–3723, 2019.

[11] B. F. Li, H. L. Zhu, B. S. Xie, L. Y. Luo, G. R. Li, and X. S. Hu, "Study on tensile properties of root soil composite of alpine meadow plants in the riparian zone of the Yellow River source region," *Chinese Journal of Rock Mechanics and Engineering*, vol. 39, no. 2, pp. 424–432, 2020.

[12] T. Liang, J. A. Knappett, A. G. Bengough, and Y. X. Ke, "Small-scale modelling of plant root systems using 3D printing, with applications to investigate the role of vegetation on earthquake-induced landslides," *Landslides*, vol. 14, no. 5, pp. 1747–1765, 2017.

[13] Y. B. Liu, X. S. Hu, D. M. Yu, S. X. Li, and Y. Q. Yang, "Microstructural features and friction characteristics of the interface of shrub roots and soil in loess area of Xining Basin," *Chinese Journal of Rock Mechanics and Engineering*, vol. 37, no. 5, pp. 1270–1280, 2018.

[14] T. H. Wu, W. P. Mckinnell, and D. N. Swanston, "Strength of tree roots and landslides on Prince of Wales Island, Alaska," *Canadian Geotechnical Journal*, vol. 16, no. 1, pp. 19–33, 1979.

[15] C. C. Fan, "A displacement-based model for estimating the shear resistance of root-permeated soils," *Plant and Soil*, vol. 355, no. 1-2, pp. 103–119, 2012.

[16] T. Liang, J. A. Knappett, A. Leung, A. Carnaghan, A. G. Bengough, and R. Zhao, "Critical evaluation of predictive models for rooted soil strength with application to predicting the seismic deformation of rooted slopes," *Landslides*, vol. 17, no. 1, pp. 93–109, 2020.

[17] C. C. Fan and H. M. Tsai, "Spatial distribution of plant root forces in root-permeated soils subject to shear," *Soil and Tillage Research*, vol. 156, pp. 1–15, 2016.

[18] Y. Kong, A. Zhou, F. Shen, and Y. Yao, "Stress–dilatancy relationship for fiber-reinforced sand and its modeling," *Acta Geotechnica*, vol. 14, no. 6, pp. 1871–1881, 2019.

[19] J. L. Ding, F. N. Dang, and S. H. Wang, "A simple model for estimating shear strength of root soil composite," *Proceedings of China-Europe Conference on Geotechnical Engineering*, vol. 3, pp. 1264–1268, 2018.

[20] M. Burylo, C. Hudek, and F. Rey, "Soil reinforcement by the roots of six dominant species on eroded mountainous marly slopes (Southern Alps, France)," *Fuel &Energy Abstracts*, vol. 84, no. 1, p. 70, 2010.

[21] K. W. Loades, A. G. Bengough, M. F. Bransby, and P. D. Hallett, "Planting density influence on fibrous root reinforcement of soils," *Ecological Engineering*, vol. 36, no. 3, pp. 276–284, 2010.

[22] W. Wen, G. F. Li, W. Hu, H. J. Liu, and W. Xiang, "Modification of reinforcement effect model of herbs root system in soil," *Chinese Journal of Rock Mechanics and Engineering*, vol. 35, no. S2, pp. 4211–4217, 2016.

[23] W. H. Zhang, G. Y. Wang, S. H. Hu, Y. J. Zhang, P. Quan, and J. M. Chang, "Indoor experimental study on the root pullout resistance of thin-leaved alum," *China Soil and Water Conservation Science*, vol. 18, no. 3, pp. 22–30, 2020.

[24] X. Xia, Y. J. Jiang, L. J. Su, and J. J. Mehtab Alam, "A model for estimating the ultimate value of shear strength of soils with roots based on interfacial cohesion," *Rock and Soil Mechanics*, vol. 42, no. 8, pp. 2173–2184, 2021.

[25] C. C. Fan and C. F. Su, "Role of roots in the shear strength of root-reinforced soils with high moisture content," *Ecological Engineering*, vol. 33, no. 2, pp. 157–166, 2008.

[26] H. Guo, L. X. Tang, Q. H. Dai, L. Pan, and S. H. Ruan, "Effect of soil particle size on root soil friction characteristics of

shrubs," *Journal of Soil and Water Conservation*, vol. 35, no. 6, pp. 83–87+94, 2021.

[27] Q. Zhang, J. Liu, Q. Li, X. Sun, J. W. Pang, and X. Zhang, "Friction characteristics of Artemisia annua and silty sand root soil and soil interface," *Northwest Agricultural Journal*, vol. 28, no. 3, pp. 489–496, 2019.

[28] Z. Y. Xia, Q. Liu, W. N. Xu, Y. K. Rao, and H. Zhang, "Characteristics of friction at the interface between root system and soil of multiflora woodland blue," *Journal of Soil and Water Conservation*, vol. 32, no. 1, pp. 128–134, 2018.

[29] R. L. Ge, Y. Q. Liu, Z. Y. Zou, H. Ar, and R. S. Na, "Effect of soil moisture on interaction characteristics of plant root soil interface," *Journal of Soil and Water Conservation*, vol. 32, no. 1, pp. 135–140, 2018.

[30] Y. Su, J. Liu, H. Li, X. Zhang, X. S. Li, and D. D. Zhou, "Effect of soil saturation on interfacial friction characteristics between Caragana korshinskii root and two kinds of soil," *Journal of Inner Mongolia Forestry Science and Technology*, vol. 43, no. 1, pp. 1–5, 2017.

[31] H. W. Xing, J. Liu, L. H. Wang et al., "Frictional properties of lemon and Salix roots at the soil and soil-soil interfaces," *Journal of Tribology*, vol. 30, no. 1, pp. 87–91, 2010.

[32] C. Zhang, X. Zhou, J. Jiang, Y. Wei, J. Ma, and P. D. Hallett, "Root moisture content influence on root tensile tests of herbaceous plants," *Catena*, vol. 172, pp. 140–147, 2019.

[33] B. Q. Lian, J. B. Peng, H. B. Zhan, and X. Wang, "Mechanical response of root-reinforced loess with various water contents," *Soil & Tillage Research*, vol. 193, pp. 85–94, 2019.

[34] O. Normaniza, H. A. Faisal, and S. S. Barakbah, "Engineering properties of Leucaena leucocephala for prevention of slope failure," *Ecological Engineering*, vol. 32, no. 3, pp. 215–221, 2008.

[35] J. Y. Li, D. M. Yu, X. Y. Zhang et al., "Experimental study on the effect of water content of slope soils on the shear strength of plant root soil complex in the loess area of Xining Basin," *Journal of Engineering Geology*, vol. 30, no. 2, pp. 281–292, 2022.

[36] M. Schwarz, F. Preti, F. Giadrossich, P. Lehmann, and D. Or, "Quantifying the role of vegetation in slope stability: a case study in Tuscany (Italy)," *Ecological Engineering*, vol. 36, no. 3, pp. 285–291, 2010.

[37] Y. Ding, Z. Y. Xia, W. N. Xu, and Q. Yang, "In-situ shear test study of substrate soil-rock contact surface under the action of root system," *Journal of Geotechnical Engineering*, vol. 38, no. 11, pp. 2107–2113, 2016.

[38] H. Xu, H. L. Yuan, X. Y. Wang, D. Wang, and J. X. C. Q. Chen, "Rong study on the influence of root morphology and hierarchical structure on the mechanical properties of root-soil complexes," *Journal of Geotechnical Engineering*, vol. 44, no. 5, pp. 926–935, 2022.

[39] Y. Ding, Z. Y. Xia, W. N. Xu, and Q. Yang, "In-situ shear test of soil-rock interface under root action," *Chinese journal of geotechnical engineering*, vol. 38, no. 11, pp. 2107–2113, 2016.